JOURNAL OF
Applied Polymer
SCIENCE

Special Issue: Polymers for Microelectronics

Guest Editors: Dr Brian Knapp (Promerus LLC) and
Prof. Paul A. Kohl (Georgia Institute of Technology)

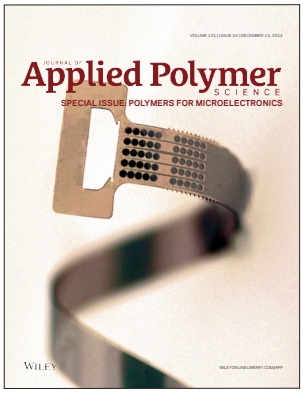

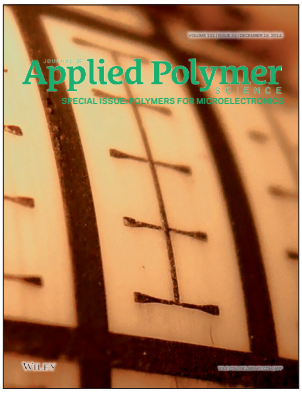

EDITORIAL

Polymers for Microelectronics
B. Knapp and P. A. Kohl, *J. Appl. Polym. Sci.* 2014, **DOI: 10.1002/app.41233**

REVIEW

Negative differential conductance materials for flexible electronics
A. Nogaret, *J. Appl. Polym. Sci.* 2014, **DOI: 10.1002/app.40169**

RESEARCH ARTICLES

Generic roll-to-roll compatible method for insolubilizing and stabilizing conjugated active layers based on low energy electron irradiation
M. Helgesen, J. E. Carlé, J. Helt-Hansen, A. Miller, and F. C. Krebs, *J. Appl. Polym. Sci.* 2014, **DOI: 10.1002/app.40795**

Selective etching of polylactic acid in poly(styrene)-block-poly(D,L)lactide diblock copolymer for nanoscale patterning
C. Cummins, P. Mokarian-Tabari, J. D. Holmes, and M. A. Morris, *J. Appl. Polym. Sci.* 2014, **DOI: 10.1002/app.40798**

Preparation and dielectric behavior of polyvinylidene fluoride composite filled with modified graphite nanoplatelet
P. Xie, Y. Li, and J. Qiu, *J. Appl. Polym. Sci.* 2014, **DOI: 10.1002/app.40229**

Design of a nanostructured electromagnetic polyaniline–Keggin iron–clay composite modified electrochemical sensor for the nanomolar detection of ascorbic acid
R. V. Lilly, S. J. Devaki, R. K. Narayanan, and N. K. Sadanandhan, *J. Appl. Polym. Sci.* 2014, **DOI: 10.1002/app.40936**

Synthesis and characterization of novel phosphorous-silicone-nitrogen flame retardant and evaluation of its flame retardancy for epoxy thermosets
Z.-S. Li, J.-G. Liu, T. Song, D.-X. Shen, and S.-Y. Yang, *J. Appl. Polym. Sci.* 2014, **DOI: 10.1002/app.40412**

Electrical percolation behavior and electromagnetic shielding effectiveness of polyimide nanocomposites filled with carbon nanofibers
L. Nayak, T. K. Chaki, and D. Khastgir, *J. Appl. Polym. Sci.* 2014, **DOI: 10.1002/app.40914**

Morphological influence of carbon modifiers on the electromagnetic shielding of their linear low density polyethylene composites
B. S. Villacorta and A. A. Ogale, *J. Appl. Polym. Sci.* 2014, **DOI: 10.1002/app.41055**

Electrical and EMI shielding characterization of multiwalled carbon nanotube/polystyrene composites
V. K. Sachdev, S. Bhattacharya, K. Patel, S. K. Sharma, N. C. Mehra, and R. P. Tandon, *J. Appl. Polym. Sci.* 2014, **DOI: 10.1002/app.40201**

Anomalous water absorption by microelectronic encapsulants due to hygrothermal-induced degradation
M. van Soestbergen and A. Mavinkurve, *J. Appl. Polym. Sci.* 2014, **DOI: 10.1002/app.41192**

Design of cyanate ester/azomethine/ZrO_2 nanocomposites high-k dielectric materials by single step sol-gel approach
M. Ariraman, R. Sasi Kumar and M. Alagar, *J. Appl. Polym. Sci.* 2014, **DOI: 10.1002/app.41097**

Furan/imide Diels–Alder polymers as dielectric materials
R. G. Lorenzini and G. A. Sotzing, *J. Appl. Polym. Sci.* 2014, **DOI: 10.1002/app.40179**

High dielectric constant polyimide derived from 5,5'-bis[(4-amino) phenoxy]-2,2'-bipyrimidine
X. Peng, Q. Wu, S. Jiang, M. Hanif, S. Chen, and H. Hou, *J. Appl. Polym. Sci.* 2014, **DOI: 10.1002/app.40828**

The influence of rigid and flexible monomers on the physical-chemical properties of polyimides
T. F. da Conceição and M. I. Felisberti, *J. Appl. Polym. Sci.* 2014, **DOI: 10.1002/app.40351**

JOURNAL OF
Applied Polymer
SCIENCE

Special Issue: Polymers for Microelectronics

Guest Editors: Dr Brian Knapp (Promerus LLC) and
Prof. Paul A. Kohl (Georgia Institute of Technology)

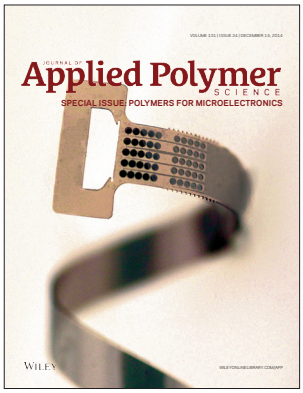

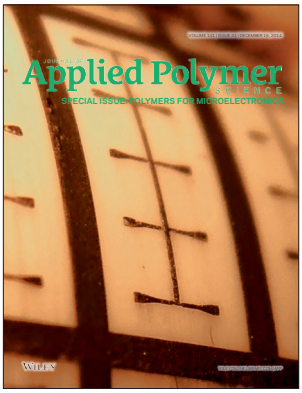

Development of polynorbornene as a structural material for microfluidics and flexible BioMEMS
A. E. Hess-Dunning, R. L. Smith, and C. A. Zorman, *J. Appl. Polym. Sci.* 2014, **DOI:** 10.1002/app.40969

A thin film encapsulation layer fabricated via initiated chemical vapor deposition and atomic layer deposition
B. J. Kim, D. H. Kim, S. Y. Kang, S. D. Ahn, and S. G. Im, *J. Appl. Polym. Sci.* 2014, **DOI:** 10.1002/app.40974

Surface relief gratings induced by pulsed laser irradiation in low glass-transition temperature azopolysiloxanes
V. Damian, E. Resmerita, I. Stoica, C. Ibanescu, L. Sacarescu, L. Rocha, and N. Hurduc, *J. Appl. Polym. Sci.* 2014, **DOI:** 10.1002/app.41015

Polymer-based route to ferroelectric lead strontium titanate thin films
M. Benkler, J. Hobmaier, U. Gleißner, A. Medesi, D. Hertkorn, and T. Hanemann, *J. Appl. Polym. Sci.* 2014, **DOI:** 10.1002/app.40901

The influence of dispersants that contain polyethylene oxide groups on the electrical resistivity of silver paste
T. H. Chiang, Y.-F. Chen, Y. C. Lin, and E. Y. Chen, *J. Appl. Polym. Sci.* 2014, **DOI:** 10.1002/app.41183

Quantitative investigation of the adhesion strength between an SU-8 photoresist and a metal substrate by scratch tests
X. Zhang, L. Du, and M. Zhao, *J. Appl. Polym. Sci.* 2014, **DOI:** 10.1002/app.41108

Thermodynamic and kinetic aspects of defectivity in directed self-assembly of cylinder-forming diblock copolymers in laterally confining thin channels
B. Kim, N. Laachi, K. T. Delaney, M. Carilli, E. J. Kramer, and G. H. Fredrickson, *J. Appl. Polym. Sci.* 2014, **DOI:** 10.1002/app.40790

Journal of Applied Polymer Science

Generic Roll-to-Roll Compatible Method for Insolubilizing and Stabilizing Conjugated Active Layers Based on Low Energy Electron Irradiation

Martin Helgesen,[1] Jon E. Carlé,[1] Jakob Helt-Hansen,[2] Arne Miller,[2] Frederik C. Krebs[1]
[1]DTU Energy Conversion, Technical University of Denmark, Frederiksborgvej 399, DK-4000 Roskilde, Denmark
[2]DTU Nutech, Technical University of Denmark, Frederiksborgvej 399, DK-4000 Roskilde, Denmark
Correspondence to: F. C. Krebs (E-mail: frkr@dtu.dk)

ABSTRACT: Irradiation of organic multilayer films is demonstrated as a powerful method to improve several properties of polymer thin films and devices derived from them. The chemical cross-linking that is the direct result of the irradiation with ~100 keV electrons is fast and has a penetration power compatible with thin plastic foils of one to two hundreds of microns typical of devices explored in organic electronics. We demonstrate here that active layers and complete devices can be subjected to electron irradiation-induced cross-linking thus facilitating multilayer solvent processing and morphological stability. The method is fast, generic, contactless, and fully compatible with high-speed roll-to-roll processing of i.e. polymer solar cells at web speeds in excess of 60 m min^{-1}. We employ fully printed, flexible, and foil-based indium-tin-oxide free polymer solar cells in this study to demonstrate the technique. We also demonstrate that polymer solar cells are exceptionally stable towards ionizing radiation and find that doses as high as 100 kGy can be used before any significant decrease in performance is observed. © 2014 Wiley Periodicals, Inc. J. Appl. Polym. Sci. **2014**, *131*, 40795.
Together with Mokarian-Tabari *et al.*, *J. Appl. Polym. Sci.* (2014) **131**, 40798, doi:10.1002/app.40798, this article is part of a Special Issue on Polymers for Microelectronics. The remaining articles appear in *J. Appl. Polym. Sci.* (2014) volume **131**, issue 24. This note was added on 1st July 2014.

KEYWORDS: conducting polymers; manufacturing; morphology

Received 28 February 2014; accepted 4 April 2014
DOI: 10.1002/app.40795

INTRODUCTION

The research within polymer solar cells (PSC) has increased during the last decade[1] because of their potential as a low-cost alternative to the inorganic solar cells. A fast increase in power conversion efficiency (PCE) has been achieved through mainly device optimization and development of new polymer/acceptor systems with improved properties.[2] High performing PSCs generally rely on the bulk hetero-junction (BHJ) structure where the polymer/acceptor mixture in the active layer have micro-phase segregated to form a bi-continuous structure with channels for both electron and hole transport. A key issue is that the excitons formed upon light irradiation have a limited diffusion length in these materials of 10–20 nm, which means that this is also the optimal physical dimensions of the domains in the hetero-junction. Unfortunately, this is not usually the thermodynamic equilibrium (i.e. the morphology of the material mixture is metastable), which is manifested in a growth of PCBM acceptor crystallites leading to destruction of the optimal morphology causing a decrease in the device performance.[3–5] To maintain the high performance one needs to stabilize the optimal morphology. Several approaches have been applied in order to preserve the optimal morphology over time.[6] One approach has been to apply side chains to the polymer with tertiary ester groups that by thermal treatment of the processed films can be cleaved off. The residual carboxylic acid groups can then form hydrogen bonds resulting in a rigid matrix that also immobilizes the acceptor part.[7] Still another strategy is to incorporate cross-linkable groups in some of the polymer side chains. The idea is once again that the cross-linking should immobilize the structure and inhibit further growth of domains. A number of different photo-curable groups have been applied for this purpose such as oxetane groups,[8] alkylbromide,[9,10] azide[11] and vinyl.[12] Common to these approaches is that additional synthetic steps have to be performed in order to incorporate the active sites for cross-linking.[13] Quite often these extra active sites present entirely different morphologies and thus represent a material that is entirely different from the champion material. Good examples of this at the two extremes are polymers based on 3-(hex-5-en-1-yl)thiophene, 3-(6-bromohexyl) thiophene, and 33-(6-azidohexyl)thiophene demonstrating little perturbation of the chemical structure as compared to the parent 3-hexylthiophene, whereas the oxetane-functionalized 3-hexylthiophene is an entirely different material. An elegant strategy to avoid

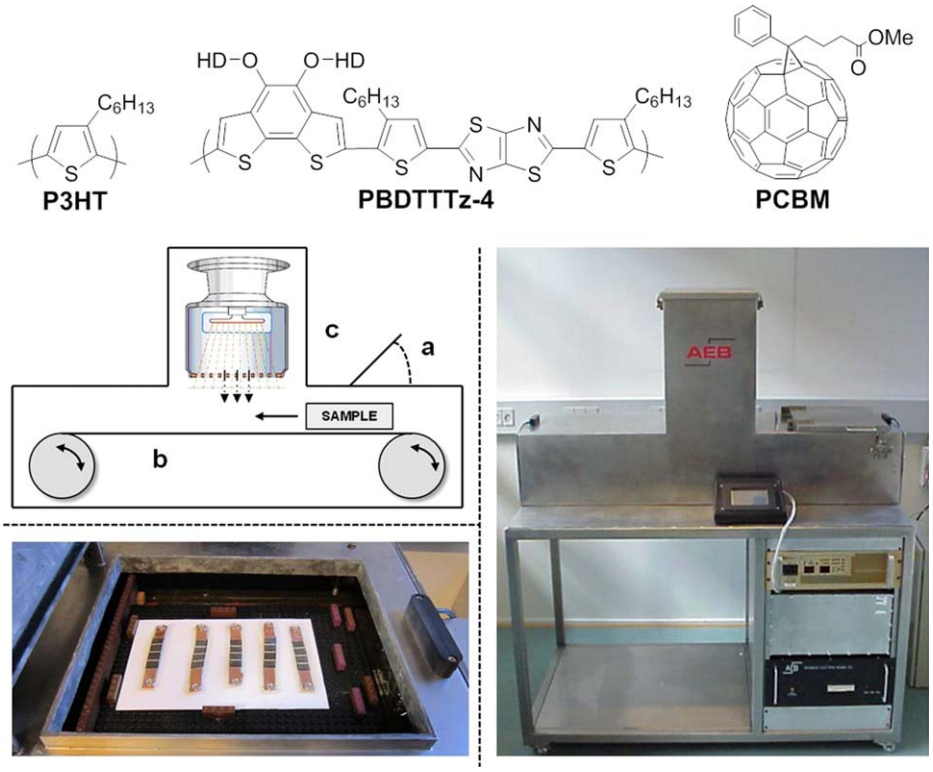

Figure 1. Top: Molecular structure of the polymers P3HT, PBDTTTz-4, and PCBM. PV-D4610 is Merck proprietary and its molecular structure is therefore not shown. HD = 2-hexyldecyl. Middle left: Schematic drawing of the electron accelerator equipment. (a) A hacth that allows placement of samples, (b) a conveyor that transports the samples past the beam window, and (c) the Risø HDRL low energy electron accelerator. Right: Picture of the electron accelerator. Bottom left: Placement of the solar cell modules on the conveyor just before an experiment. [Color figure can be viewed in the online issue, which is available at wileyonlinelibrary.com.]

that cross-linkage has to be chemically engineered into the material is the use of electron irradiation which is already an established technology that can be implemented in large scale fabrication of PSCs with relative simplicity.

In this work we report on the use of electron irradiation as a method for cross-linking the active layer of PSCs together with stabilization of the device performance of flexible indium-tin-oxide-free PSC modules. Three different polymers were applied in this study, P3HT, PV-D4610, and PBDTTTz-4, that all have shown high PCE in roll coated processing (PCE of 2–3%) but with variation in device durability.[14] The electron irradiation generates active sites in the materials of the device, among others the active layer, which allows for the cross-linking to take place. The method is therefore generic for all polymers and no additional chemical modifications will have to be performed for achieving cross-linking and stabilization once the optimized processing conditions have been attained it is a straightforward and non-invasive process. An absorbed dose in the range of 10–500 kGy were applied and the effect of irradiation on the active layer was studied using solvent resistance tests, UV-vis, and optical microscopy. Additionally, the effect of irradiation on the operational durability of completed encapsulated devices was studied in the dark at elevated temperature.

EXPERIMENTAL

A substrate consisting of barrier-foil/Ag grid/high conducting PEDOT : PSS/ZnO was fabricated in the form of 10 mm wide stripes by R2R processing following a previously reported procedure.[15] The active layer, consisting of either P3HT : PCBM (1 : 1, by weight) in chlorobenzene, PV-D4610 : PCBM (1 : 2.5, by weight) in ortho-dichlorobenzene or PBDTTTz-4 : PCBM (1 : 2, by weight) in chlorobenzene : ortho-dichlorobenzene (4 : 1, by volume), with a concentration of 40 mg mL^{-1} was slot-die coated at 70°C (60°C for P3HT:PCBM) with an offset of 2 mm from the Ag grid/PEDOT : PSS/ZnO electrode enabling electrical contact to be made to the front electrode. The flow of the solution was in the range of 0.1–0.2 ml min^{-1} and the web speed in the range of 0.8–1.3 m min^{-1} resulting in wet thicknesses in the range of 8–12 μm. The back PEDOT : PSS (Agfa EL-P 5010 was diluted with isopropyl alcohol to 2 : 1 by weight) layer was slot-die coated on the active layer with a further offset of 1 mm with a wet thickness of 200–250 μm. The PEDOT : PSS was dried for 30 min at 80°C, before the silver back electrode was applied by flexographic printing of a heat-curing silver paste (PV410, Dupont) followed by annealing at 120°C in an oven for 5 min.

The fabricated solar cells were then divided into modules comprising four serially connected devices. The modules had an active area of ≈4 cm^2, defined by the overlap between the back PEDOT : PSS layer and the front electrode (Ag grid/PEDOT : PSS). *I–V* characteristics were measured with a Keithley 2400 source meter under 100 mW cm^{-2} white light from a Steuernagel solar simulator.

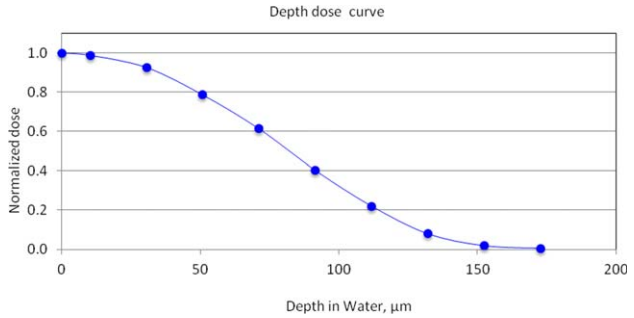

Figure 2. Depth dose curve for 125 keV electrons measured at the Risø High-Dose Reference Laboratory accelerator. [Color figure can be viewed in the online issue, which is available at wileyonlinelibrary.com.]

Encapsulation was performed using barrier foil from Amcor and a UV curable adhesive from DELO® (DELO® – Katibobond LP 655). The modules were passed under a nip pressure in a R2R machine followed by curing of the adhesive for 2 min under a solar simulator. Cu tape (3M) was applied to the terminals before encapsulation and metal snap fasteners were then applied onto the Cu tape over the barrier layer to establish the electrical contact.

Irradiations were performed using an AEB DC-beam electron accelerator of Risø High Dose Reference Laboratory (Figure 1). The electron energy range is 80–125 keV, and beam current can be selected in the range between 1 and 10 mA. Samples are placed on a conveyor that passes the exit window. All samples and encapsulated modules were irradiated with 123 keV electrons at beam currents between 1.2 and 6 mA in order to vary the dose between 10 and 500 kGy (doses greater than 50 kGy were given as multiple irradiations). The absorbed dose to the active layer when encapsulated devices were irradiated was determined by dosimetry experiments.[16] This was achieved by placing a thin radiochromic film dosimeter at the interface between the back PEDOT and the active layer of an encapsulated module. After irradiation the dosimeter was analyzed using a flatbed scanner (Epson Perfection 3170) and RisøScan software,[17] which showed that approximately 50% of the radiation penetrates into the active layer, see Figure 2.

The encapsulated devices were irradiated through the back side, i.e. barrier foil and back PEDOT that was measured to have a thickness around 70 μm.

RESULTS AND DISCUSSION

Cross-Linking of the Active Layer

Thin films of the three polymers blended with PCBM were slot-die coated on a clear PET substrate followed by annealing at 120°C for 5 min in an oven. The substrates were divided into several smaller pieces and irradiated with doses ranging from 10 to 500 kGy. An absorption profile was recorded of each sample together with a pristine sample in order to study the effect of irradiation on the optical properties of the active layer (Figure 3). This shows that the samples can withstand irradiation doses up to approximately 200 kGy before a significant change of the absorption profile is observed.

For the P3HT : PCBM films the characteristic shoulder around 580 nm [Figure 3(a)] starts to disappear when the film is irradiated with 200 kGy and when the dose is increased to 500 kGy the absorption band in the range of 400–600 nm is flattening/blue shifting, indicating degradation of the conjugated backbone. The absorption band at 600 nm in PBDTTTz-4 : PCBM films [Figure 3(b)] loose intensity along with increasing irradiation dose which is most clearly observed for the film irradiated with 500 kGy. The same trend is observed for PV-D4610 : PCBM films [Figure 3(c)] where the absorption band at 650 nm experience a reduction in intensity as a function of

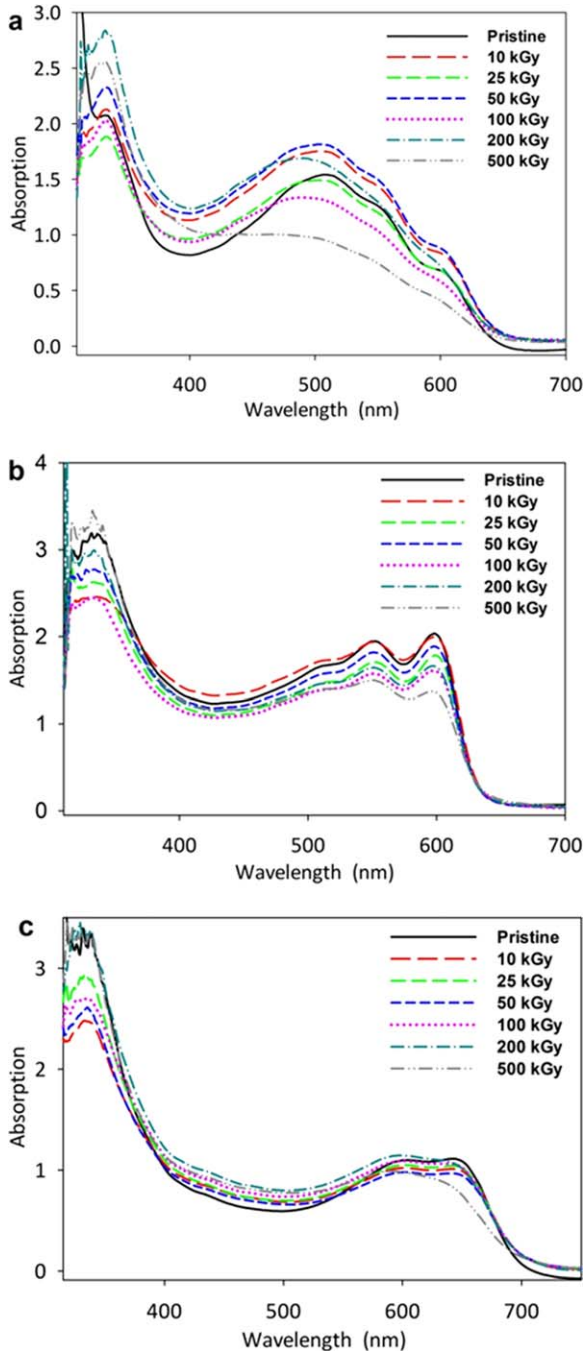

Figure 3. UV-vis absorption spectra of active layer slot-die coated on PET substrate before irradiation and after irradiation of (a) P3HT : PCBM, (b) PBDTTTz-4 : PCBM, and (c) PV-D4610 : PCBM. [Color figure can be viewed in the online issue, which is available at wileyonlinelibrary.com.]

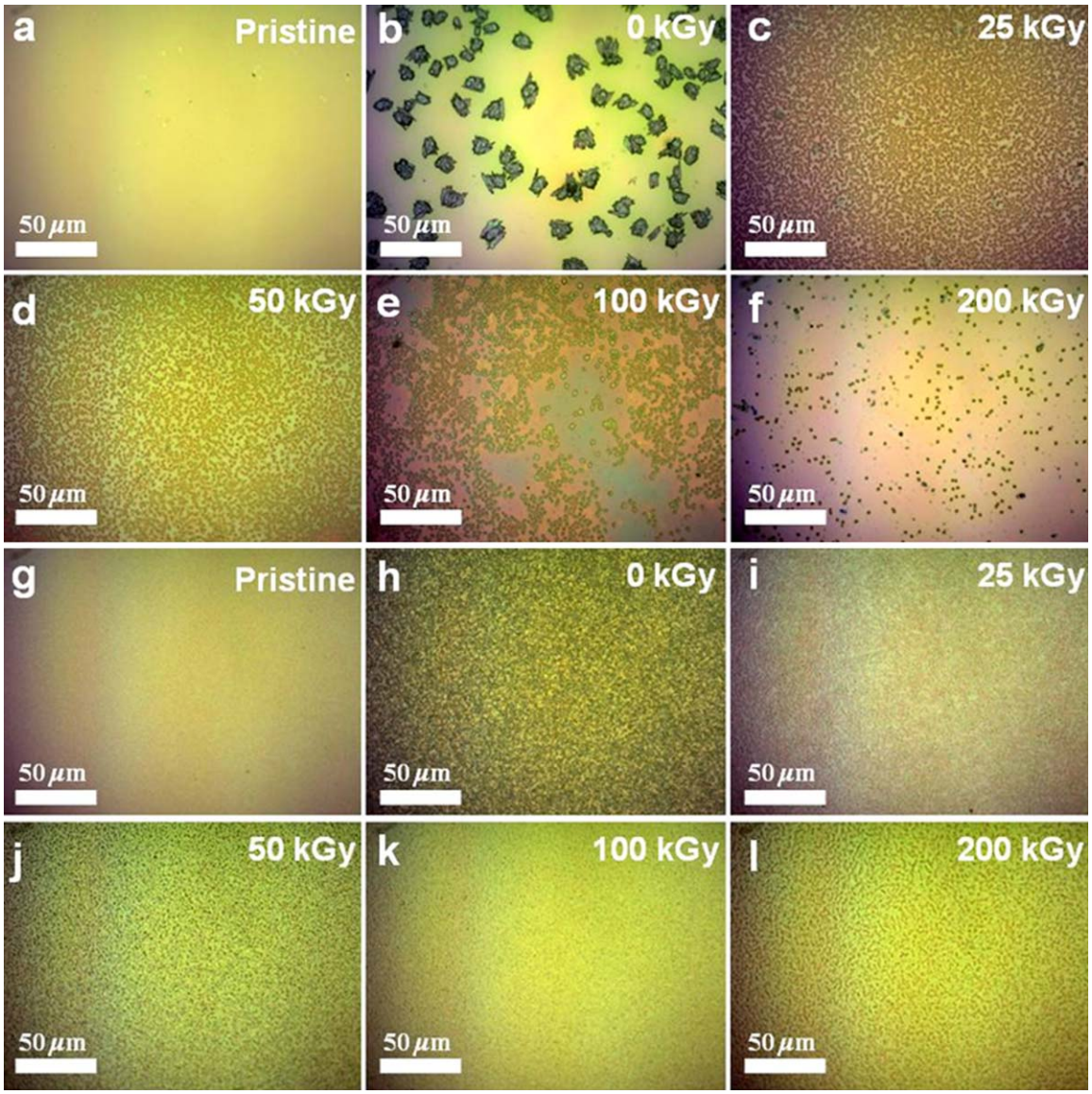

Figure 4. Optical micrographs (200 × 260 μm^2) of polymer:PCBM films after annealing at 140°C for 24 h. The samples have been irradiated in the range of 0–200 kGy before annealing. The dark areas correspond to PCBM rich domains. (a–f) P3HT : PCBM (1 : 1), (g–l) PBDTTTz-4 : PCBM 1 : 2, (m–r) PV-D4610 : PCBM 1 : 2.5. [Color figure can be viewed in the online issue, which is available at wileyonlinelibrary.com.]

increasing irradiation dose. In order to examine the effect of cross-linking on the BHJ morphology each of the irradiated polymer : PCBM samples were annealed at 140°C for 24 h. Optical microscopy images were recorded before and after annealing, see Figure 4(a–r). As expected, a large degree of noticeable microsized PCBM domains formed in the reference samples [Figure 4(b,h,n)] that had not been subjected to irradiation whereas the irradiated samples generally showed reduced macrophase segregation along with increasing irradiation dose. While elucidation of the exact mechanism of cross-linking is beyond the scope of this work it is well known that the cross-linking in organic materials is known to take place when free radicals generated during electron irradiation recombine with the formation of new bonds. In the case of our films the cross-linking sites can be either between side chains, side chains–backbones, or backbone–backbone. The majority of intermolecular contacts in our systems are between sidechains and therefore it is likely that sidechain–sidechain cross-links constitute the majority. This is also supported by the fact that a significant dose does not affect the electronic properties to a great extent which would have been expected if the backbone cross-links were dominant. Only at the very high doses do we start to see changes in the absorption spectra. Further support of this is also found in the observation that a higher fullerene loading is beneficial to the resilience towards radiation dose which corroborates well with the well-known radical scavenging properties of fullerenes. The content of PCBM in the thin films is observed to have an effect on the optical degradation of the materials applied in this work. Ex. P3HT:PCBM, which has the lowest amount of PCBM (1 : 1), shows a more pronounced change in the absorption profile (blue shift) when irradiated with doses over 200 kGy compared to ex. PV-D4610:PCBM

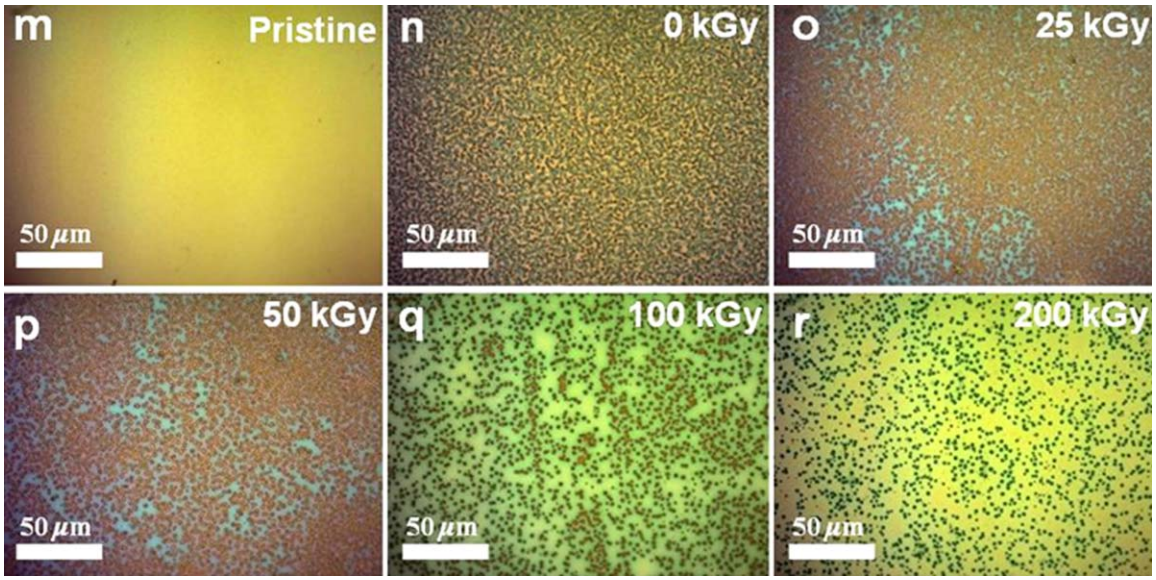

Figure 4. *Continued*

with a ratio of 1 : 2.5. These observations also transcend into the morphological stability of the films. This is most clearly observed for the P3HT : PCBM films where the film irradiated with 200kGy [Figure 4(f)] only shows a small degree of aggregation in the film which is in stark contrast to the reference sample [Figure 4(b)] where thermal annealing induces the formation of many micrometer sized crystals. This further confirms that cross-linking takes place during irradiation and that it can stabilize the nano size BHJ morphology in the active layer. In addition to enhanced thermal stability of the BHJ morphology cross-linking by irradiation also provide high solvent resistivity as can be seen in Figure 5.

There is however a balance between the positive effects upon E-beam irradiation (solvent resistance and morphological stabilization) and the negative effects on the electronics properties (optical absorption and carrier transport). The optimal dose thus has to be found in each case. Especially the solvent resistance which is induced already at low doses is particularly relevant in the context of multilayer processing using only solvent-based methods (i.e. printing and coating methods). As an extreme example of this the organic tandem solar cell that in its ultimate form may comprise well in excess of 10 wet processed layers may necessitate a simple method to control solubility of the already processed layers at one or more stages in the process.

Irradiation of PSC

Stabilization of the active layer morphology is believed to have a crucial impact on the long-term device performance.[6] Other important degradation mechanisms when applying flexible substrates compared to rigid glass substrates are delamination between the layers because of mechanical stress and poor matching of the thermomechanical properties.[18] Fully encapsulated PSC modules on flexible substrates having an inverted geometry (substrate/Ag-grid/PEDOT : PSS/ZnO/active layer/PEDOT:PSS/Ag [Figure 6(a–c)] were therefore irradiated, hereby not only cross-linking the active layer but all the layers in the devices. When wishing to employ electron irradiation to stabilize morphology the final encapsulated device can be irradiated

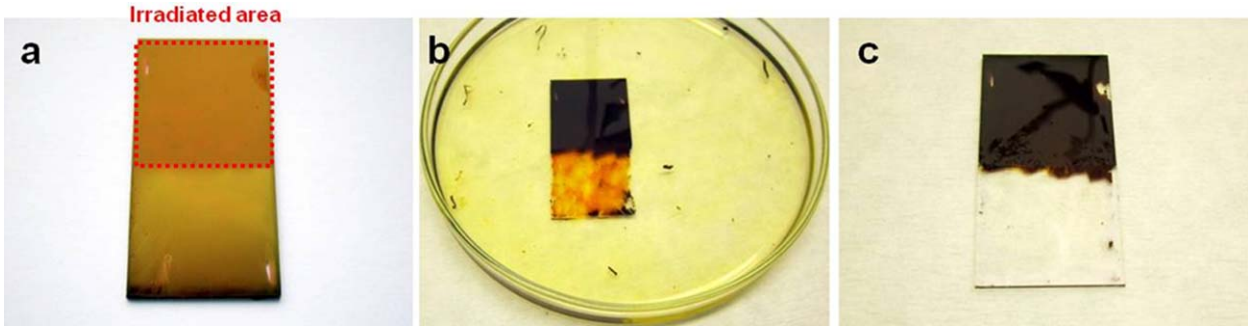

Figure 5. (a) Irradiated (25 kGy) P3HT/PCBM thin films were (b) immersed into ODCB where unirradiated film areas dissolved and washed off, (c) whereas irradiated areas remained on the substrate demonstrating a high solvent resistance because of cross-linking. The dry film is shown in (a) whereas the wet (solvent submerged) film is shown in (b) and the wet film is shown in (c). [Color figure can be viewed in the online issue, which is available at wileyonlinelibrary.com.]

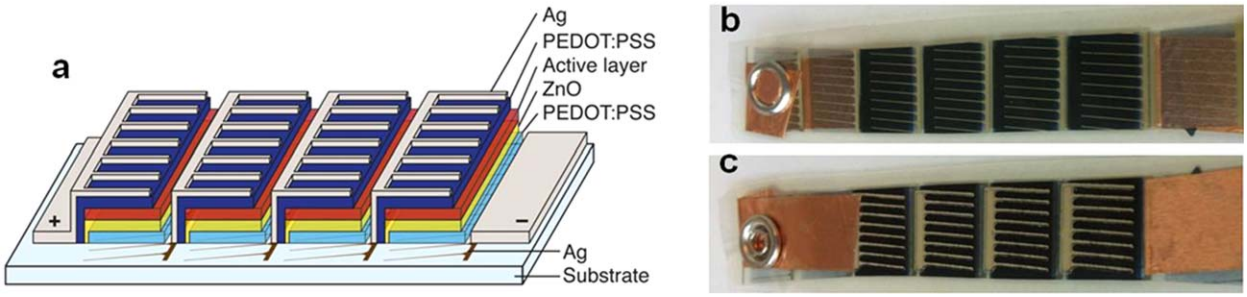

Figure 6. (a) Schematic representation of the solar cell modules consisting of four serially connected cells. Photographs of the encapsulated modules from: (b) the front side and (c) the backside. [Color figure can be viewed in the online issue, which is available at wileyonlinelibrary.com.]

thereby avoiding the presence of oxygen and water during the irradiation process which could have a damaging effect on the materials and the device functionality.

The Effect of Absorbed Dose on Device Performance

The PCE of the modules were measured before and after irradiation with doses ranging from 25 to 500 kGy, corresponding to approximately 10–250 kGy in the active layer. The changes in PCE as a result of irradiation are summarized in Figure 7 (the PCE is normalized to its value before irradiation) and Table I. Irradiation of the devices resulted in a slight decrease of the device performance. Figure 7 shows that P3HT-based devices were less affected by irradiation followed by devices based on PV-D4610, whereas devices based on PBDTTTTz-4 were most affected by irradiation. In general it is shown that applying low doses of 0–100 kGy only causes a very limited decrease of the device performance (maximally 10%). Applying a higher dose (200–500 kGy) has a much larger negative impact on the devices and a reduction in performance of 12–35% is observed depending on dose and polymer. Irradiation of the devices mainly affects the current and to a lesser extent the fill factor, whereas the voltage remains almost unaffected even at 500 kGy.

Operational Lifetime Measurements

Figure 8 shows the PCE, normalized to its value before irradiation, as a function of time during thermal annealing at 85°C (according to the ISOS-D-2 standard[19]) in the dark under an ambient atmosphere. Annealing of the devices does not reveal any clear degradation trend, when comparing the three polymers, because of thermally induced changes such as the growth of PCBM domains, interface changes and diffusion of material within the solar cell.

In the case of the devices based on P3HT:PCBM, the reference device has the same steady degradation curve as the devices irradiated with 200–500 kGy whereas the devices irradiated with 25–100 kGy show an initial decay during the first 100 h. Apparently a low dose, 25–100 kGy, can trigger a fast degradation mechanism, leading to almost complete degradation of the P3HT : PCBM devices within 500 h, whereas a higher dose, 200–500 kGy, does not. With respect to the devices based on PBDTTTz-4 : PCBM and PV-D4610 : PCBM, the reference device, together with the devices irradiated with a low dose (25–100 kGy), have a steeper degradation curve during the first 100 h, compared to the devices irradiated with a high dose (200–500 kGy) that has a more steady degradation curve over 500 h of thermal annealing.

A clear thermal stability enhancement after cross-linking by irradiation can only be observed for the devices based on PV-D4610 : PCBM. A high dose of 200 kGy, in this case, is the appropriate quantity of irradiation to ensure a functional device with good thermal stability at 85°C. Also the performance drop after irradiation (200 kGy) is negligible because it is retained/improved to the initial performance of the pristine device within 1 h of thermal annealing at 85°C (Figure 8). The general observation is that complete encapsulated devices are compatible with ~100 keV electron irradiation, with doses as high as 500 kGy, which leads to cross-linking of the materials and subsequently enhanced thermal stability of the BHJ morphology, depending on the material combination. Generally, the irradiation of the devices decreased the device performance. However, the device performance was, in most cases, retained/improved within 1 h of thermal annealing at 85°C and we believe that it

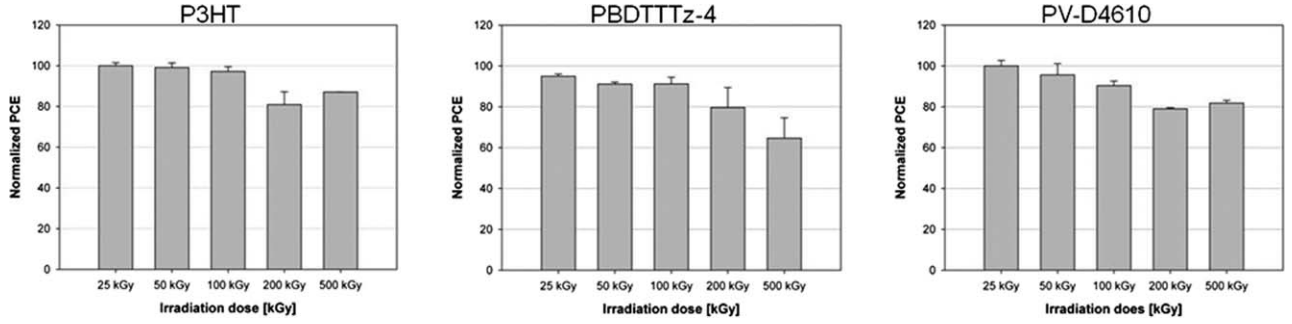

Figure 7. Change in PCE (average of three devices) as a result of irradiation dose [kGy] for the three polymers. The PCE has been normalized to its value before irradiation.

Table I. Typical Photovoltaic Parameters of Encapsulated Modules Before and After Irradiation with Different Doses

		Photovoltaic parameters before irradiation				Photovoltaic parameters after irradiation			
Device	Absorbed dose (kGy)	Voc (V)	Isc (mA)	FF (%)	PCE (%)	Voc (V)	Isc (mA)	FF (%)	PCE (%)
P3HT	25	2.1	4.3	57	1.5	2.1	4.3	58	1.5
P3HT	50	2.1	4.6	57	1.6	2.1	4.5	60	1.6
P3HT	100	2.1	4.7	60	1.7	2.1	4.6	60	1.7
P3HT	200	2.1	4.3	58	1.5	2.1	3.7	57	1.3
P3HT	500	2.1	4.1	59	1.5	2.1	3.7	56	1.3
PV-D4610	25	2.8	4.8	52	2.0	2.8	4.8	52	2.0
PV-D4610	50	2.9	4.9	49	1.9	2.9	4.9	49	1.9
PV-D4610	100	2.9	4.9	52	2.1	2.8	4.6	50	1.9
PV-D4610	200	2.9	4.6	52	2.0	2.8	3.8	50	1.5
PV-D4610	500	2.8	4.4	52	1.9	2.8	3.8	49	1.5
PBDTTTz-4	25	3.2	3.7	47	1.6	3.2	3.5	47	1.5
PBDTTTz-4	50	3.2	4.0	51	1.8	3.2	3.7	50	1.7
PBDTTTz-4	100	3.2	3.9	51	1.8	3.1	3.8	48	1.6
PBDTTTz-4	200	3.2	3.6	49	1.6	3.1	3.5	46	1.4
PBDTTTz-4	500	3.2	3.7	49	1.6	3.0	2.8	45	1.1

The modules consists of four serially connected devices with an active area of ≈3.5 cm^2.

is a matter of dose optimization, with respect to the selected materials, in order to ensure highly functional devices with enhanced thermal stability. As mentioned before, cross-linking by irradiation can also provide high solvent resistivity (Figure 5) of the active layer, thus facilitating multilayer solvent processing of e.g. tandem devices. Irradiation enables insolubilization of the deposited active films and can therefore prevent the film from being dissolved and damaged when following layers are processed on top. With regards to tandem cells, this is important as cracks in the recombination layer allows solvent from the later processed active layer, to penetrate to the first processed active layer. This can solubilize the front active layer and hence disrupt the serial connection. Because of an insoluble nature of the active materials after the irradiation step there is no limit in the choice of solvents when processing the subsequent layers in the tandem cell and forthcoming research will explore the use of low energy electron irradiation in the fabrication process of tandem devices.

CONCLUSION

In conclusion, we demonstrate that low energy electron irradiation can be used as a powerful tool to improve several properties of BHJ polymer : PCBM thin films and devices derived from them with only slight compromises made in other properties. The chemical cross-linking that is the direct result of the irradiation is fast and has a penetration power compatible with thin plastic foils of several hundreds of microns which is typical for devices explored in organic electronics. We show that active layers and complete devices, based on three donor polymers, P3HT, PV-D4610, and PBDTTTz-4 combined with the acceptor PCBM can be subjected to electron irradiation thus enhancing the thermal stability of the BHJ and the solvent resistivity. In

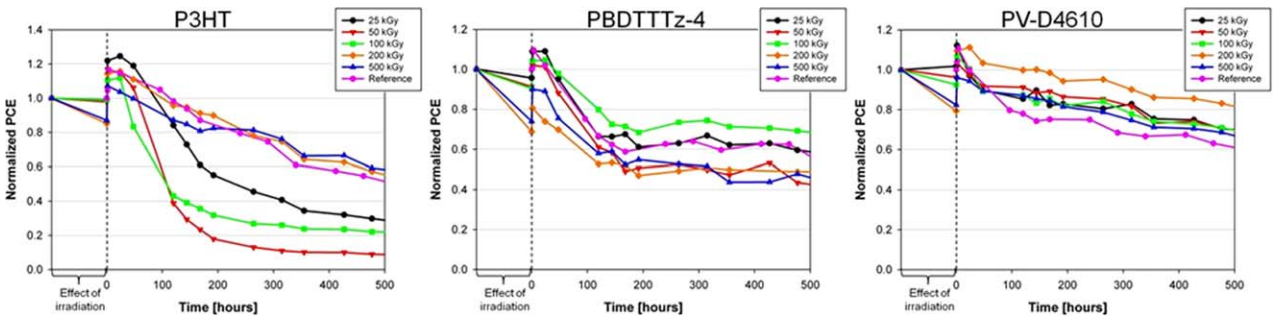

Figure 8. Normalized PCE of encapsulated modules irradiated with different doses during thermal annealing at 85°C in dark at ambient atmosphere. The PCE has been normalized to the performance of the modules before irradiation. The reference devices were not irradiated. Data shown are for one set of modules. [Color figure can be viewed in the online issue, which is available at wileyonlinelibrary.com.]

terms of optical properties, the polymer : PCBM samples can withstand irradiation doses up to approximately 200 kGy before a detectable change of the absorption profile is observed. Finally, the effect of irradiation on the operational stability of completed encapsulated devices at elevated temperature showed that the devices are compatible with irradiation doses as high as 500 kGy. A clear thermal stability enhancement after cross-linking by irradiation can be observed for the devices based on PV-D4610 : PCBM where a high dose of 200 kGy ensures a functional device with good thermal stability at 85°C. Generally, the irradiation of the devices decreased the device performance, but in most cases the performance was retained/improved within 1 h of thermal annealing. Low-energy electron irradiation, as a way of cross-linking the active layer of PSCs, is an elegant strategy to avoid that cross-linkage has to be chemically engineered into the materials. The method is fast, generic, contactless, and fully compatible with high-speed roll-to-roll processing of PSC on thin carrier substrates. Furthermore, irradiation enables insolubilization of the deposited active films thus facilitating multilayer wet processing with no restriction to the choice of solvents.

ACKNOWLEDGMENTS

This work has been supported by the Danish Council for Independent Research, Technology and Production Sciences (project nr. 11-116864) and Energinet.dk (project no. 10728 and 12144). We acknowledge support from the Office of Naval Research (Award number: N00014-11-1–0245) for the polymer synthesis, along with the fabrication and characterization of the solar cells, DFG in the frame of SPP 1355 Elementary processes in organic photovoltaics and the Danish Ministry of Science, Innovation and Higher Education under a Sapere Aude Top Scientist grant (no. DFF – 1335-00037A), and an Elite Scientist grant (no. 11-116028).

REFERENCES

1. Jørgensen, M.; Carlé, J. E.; Søndergaard, R.; Lauritzen, M.; Dagnæs-Hansen, N. A.; Byskov, S. L.; Andersen, T. R.; Larsen-Olsen, T. T.; Böttiger, A. P. L.; Andreasen, B.; Fu, L.; Zuo, L.; Liu, Y.; Bundgaard, E.; Zhan, X.; Chen, H.; Krebs, F. C. *Sol. Energy Mater.Sol. Cells.* **2013**, *119*, 84.
2. Son, H. J.; Carsten, B.; Jung, I. H.; Yu, L. *Energy Environ. Sci.* **2012**, *5*, 8158.
3. Bertho, S.; Janssen, G.; Cleij, T. J.; Conings, B.; Moons, W.; Gadisa, A.; D'Haen, J.; Goovaerts, E.; Lutsen, L.; Manca, J.; Vanderzande, D. *Sol. Energy Mater. Sol. Cells* **2008**, *92*, 753.
4. Drees, M.; Hoppe, H.; Winder, C.; Neugebauer, H.; Sariciftci, N. S.; Schwinger, W.; Schäffler, F.; Topf, C.; Scharber, M. C.; Zhu, Z.; Gaudiana, R. *J. Mater. Chem.* **2005**, *15*, 5158.
5. Moon, J. S.; Lee, J. K.; Cho, S.; Byun, J.; Heeger, A. J. *Nano Lett.* **2009**, *9*, 230.
6. Bundgaard, E.; Helgesen, M.; Carlé, J. E.; Krebs, F. C.; Jørgensen, M. *Macromol. Chem. Phys.* **2013**, *214*, 1546.
7. Liu, J. S.; Kadnikova, E. N.; Liu, Y. X.; McGehee, M. D.; Fréchet, J. M. J. *J. Am. Chem. Soc.* **2004**, *126*, 9486.
8. Farinhas, J.; Ferreira, Q.; Di Paolo, R. E.; Alcáer, L.; Morgado, J.; Charas, A. *J. Mater. Chem.* **2011**, *21*, 12511.
9. Kim, B. J.; Miyamoto, Y.; Ma, B.; Fréchet, J. M. J. *Adv. Funct. Mater.* **2009**, *19*, 2273.
10. Griffini, G.; Douglas, J. D.; Piliego, C.; Holcombe, T. W.; Turri, S.; Fréchet, J. M. J.; Mynar, J. L. *Adv. Mater.* **2011**, *23*, 1660.
11. Nam, C. Y.; Qin, Y.; Park, Y. S.; Hlaing, H.; Lu, X.; Ocko, B. M.; Black, C. T.; Grubbs, R. B. *Macromolecules* **2012**, *45*, 2338.
12. Lee, R. H.; Syu, J. Y.; Huang, J. L. *Polym. Adv. Technol.* **2011**, *22*, 2110.
13. Carlé, J. E.; Andreasen, B.; Tromholt, T.; Madsen, M. V.; Norrman, K.; Jørgensen, M.; Krebs, F. C. *J. Mater. Chem.* **2012**.
14. Carlé, J. E.; Helgesen, M.; Madsen, M. V.; Bundgaard, E.; Krebs, F. C. *J. Mater. Chem. C* **2014**, *2*, 1290.
15. Hösel, M.; Søndergaard, R. R.; Jørgensen, M.; Krebs, F. C. *Energy Technol.* **2013**, *1*, 102.
16. Helt-Hansen, J.; Miller, A.; Sharpe, P. *Radiat. Phys. Chem.* **2005**, *74*, 341.
17. Helt-Hansen, J.; Miller, A.; McEwen, M.; Sharpe, P.; Duane, S. *Radiat. Phys. Chem.* **2004**, *71*, 355.
18. Krebs, F. C.; Jørgensen, M.; Norrman, K.; Hagemann, O.; Alstrup, J.; Nielsen, T. D.; Fyenbo, J.; Larsen, K.; Kristensen, J. *Sol. Energy Mater. Sol. Cells* **2009**, *93*, 422.
19. Reese, M. O.; Gevorgyan, S. A.; Jørgensen, M.; Bundgaard, E.; Kurtz, S. R.; Ginley, D. S.; Olson, D. C.; Lloyd, M. T.; Morvillo, P.; Katz, E. A.; Elschner, A.; Haillant, O.; Currier, T. R.; Shrotriya, V.; Hermenau, M.; Riede, M.; Kirov, R.; Trimmel, G.; Rath, T.; Inganäs, O.; Zhang, F.; Andersson, M.; Tvingstedt, K.; Lira-Cantu, M.; Laird, D.; McGuiness, C.; Gowrisanker, S.; Pannone, M.; Xiao, M.; Hauch, J.; Steim, R.; DeLongchamp, D. M.; Rösch, R.; Hoppe, H.; Espinosa, N.; Urbina, A.; Yaman-Uzunoglu, G.; Bonekamp, J. B.; van Breemen, A. J. J. M.; Girotto, C.; Voroshazi, E.; Krebs, F. C. *Sol. Energy Mater. Sol. Cells* **2011**, *95*, 1253.